AIAA JOURNAL
Vol. 46, No. 1, January 2008

Aerospace Letters

AEROSPACE LETTERS are brief communications (approximately 2000 words) that describe new and potentially important ideas or results, including critical analytical or experimental observations that justify rapid publication. They are stringently prescreened, and only a few are selected for rapid review by an Editor. They are published as soon as possible electronically and then appear in the print version of the journal.

Development of High-Spectral-Resolution Planar Laser-Induced Fluorescence Imaging Diagnostics for High-Speed Gas Flows

Waruna D. Kulatilaka,* Sameer V. Naik,† and Robert P. Lucht‡
Purdue University, West Lafayette, Indiana 47907-2088

DOI: 10.2514/1.34971

Introduction

IN THIS Letter, we describe planar laser-induced fluorescence imaging (PLIF) of nitric oxide (NO) using an injection-seeded, tunable, pulsed optical parametric (OP) system. By using multiple high-resolution laser pulses tuned to precise frequency positions in the NO spectral line shape, measurements of pressure, temperature, and velocity were obtained in a supersonic underexpanded jet flowfield. The use of our high-resolution OP system is critical for obtaining this thermodynamic information, because the spectral width of the tunable pulsed laser radiation is much smaller than the spectral width of the molecular resonance, even at low pressures.

Supersonic and hypersonic flows involve strong coupling between kinematic and thermochemical states. Complete characterization of such flows requires advanced laser diagnostics for simultaneous optical measurement of instantaneous kinematic and thermochemical properties with sufficient spatial resolution and sample size. The use of high-resolution LIF for measurement of velocity, pressure, and temperature in hypersonic helium flows was first demonstrated by Zimmerman and Miles [1]. The flow was seeded with vapor-phase sodium and a continuous-wave (cw) ring dye laser was scanned over the sodium D_2 resonance features. Hiller et al. [2] used a cw ring dye laser to perform velocity imaging measurements in a subsonic jet flow seeded with iodine. McDaniel et al. [3] used an argon-ion laser tuned over a small frequency range to perform velocity measurements in a supersonic underexpanded jet flow seeded with iodine. Paul et al. [4] used a frequency-doubled pulsed dye laser with a relatively broad spectral width to perform instantaneous PLIF velocity imaging measurements in an underexpanded jet flow seeded with nitric oxide. Velocity and thermodynamic information can also be obtained using filtered Rayleigh scattering as well as molecular filter-based velocimetry [5,6]. Stimulated Raman spectroscopy [7], inverse Raman spectroscopy [8], and coherent anti-Stokes Raman scattering (CARS) [9,10] have also been used for such measurements in supersonic flows.

Although the measurements that we have performed are not instantaneous, the laser system that we have developed is ideal for instantaneous high-resolution LIF imaging measurements when combined with emerging pulse-burst laser technology [11–13]. The solid-state OP system can be pumped at much higher repetition rates than dye lasers, in which bleaching of the gain medium limits the repetition rate of the pump source. The OP system that we have developed is injection-seeded with a near-infrared telecommunications diode laser; this seed laser can be tuned rapidly so that the frequency can be tuned over the resonance line shape in less than 10 μs. The use of the OP system pumped by a pulse-burst laser in conjunction with MHz-rate framing cameras [13] could potentially allow instantaneous PLIF measurements of kinematic and thermochemical properties in supersonic and hypersonic flows.

Experimental System and Procedure

Figure 1 shows a schematic diagram of the OP system. Similar injection-seeded OP systems developed by our group have been described in detail in a previous publication [14]. Briefly, an optical parametric generator (OPG) consisting of two counter-rotating beta-barium-borate (β-BBO) crystals is pumped using the third harmonic output of an injection-seeded Nd:YAG laser. The OPG is injection-seeded at 1652 nm using a near-infrared distributed feedback (DFB) diode laser to generate pulsed signal radiation at 452 nm. An optical parametric oscillator (OPO) cavity is formed by placing two mirrors around the OPG stage. These mirrors are highly reflective at the signal wavelength but nearly completely transmissive at the idler wavelength. The signal radiation generated in the OPO stage is then amplified using an optical parametric amplifier (OPA) stage, consisting of four β-BBO crystals. The OPA is pumped by the third harmonic output of the same Nd:YAG laser. The OPO/OPA system generates approximately 20 mJ/pulse of 452-nm radiation having nearly Fourier-transform-limited bandwidth of 220 MHz. The 452-nm beam is frequency-doubled to generate approximately 1.5 mJ/pulse of ultraviolet (UV) radiation around 226 nm to excite transitions in the $A^2\Sigma^+$–$X^2\Pi$ electronic system of NO. To avoid saturation effects in the PLIF signal, neutral density filters are used to reduce the UV energy to about 0.5 mJ/pulse.

High-pressure gas flowed through a solenoid valve before exiting from a specially contoured convergent nozzle (exit diameter $D = 5$ mm) to produce a highly underexpanded jet. The jet

Received 4 October 2007; accepted for publication 13 October 2007.

*Currently Postdoctoral Research Associate, Combustion Research Facility, Sandia National Laboratories, Livermore, CA. Member AIAA.

†Senior Research Associate, School of Mechanical Engineering. Member AIAA.

‡Professor, School of Mechanical Engineering, Room 86, Mechanical Engineering Building, 585 Purdue Mall; lucht@ecn.purdue.edu. Associate Fellow AIAA (Corresponding Author).

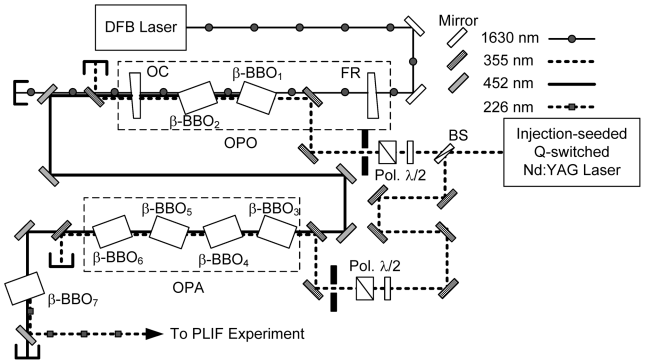

Fig. 1 Injection-seeded optical parametric system for high-resolution NO-PLIF imaging of an underexpanded supersonic jet using an OPO/OPA system; BS: beam splitter, FR: full reflector, λ/2: half-wave plate, OC: output coupler, and Pol: Polarizer.

stagnation pressure was approximately 6 atm. The gas was nitrogen seeded with 300 ppm of NO. The UV radiation near 226 nm was formed into a sheet using a cylindrical lens and focused above the nozzle exit using a spherical lens. A quartz calibration cell filled with 300-ppm NO in N_2 at room temperature and pressure was placed in the path of the laser sheet just before the nozzle exit such that PLIF images of the calibration cell and nozzle flowfield could be recorded using the same camera. The UV wavelength was tuned over the $Q_2(5) + Q_{12}(5)$ transition in the $\gamma(0,0)$ band of NO by precisely scanning the temperature of the DFB seed laser of the OPO/OPA system. The opening of the solenoid valve and the camera shutter were synchronized with the laser pulse using LabVIEW. At each wavelength, a PLIF image was acquired using a CCD camera (Andor model MCD, DU-440) having approximately 25% quantum efficiency near 226 nm. In the first set of experiments, the nozzle was set such that the flow direction and the UV laser sheet were perpendicular (90-deg case; see Fig. 2). A second set of experiments was performed by tilting the nozzle such that the laser sheet intersected the flow at 45 deg with respect to the vertical axis (45-deg case; see Fig. 2).

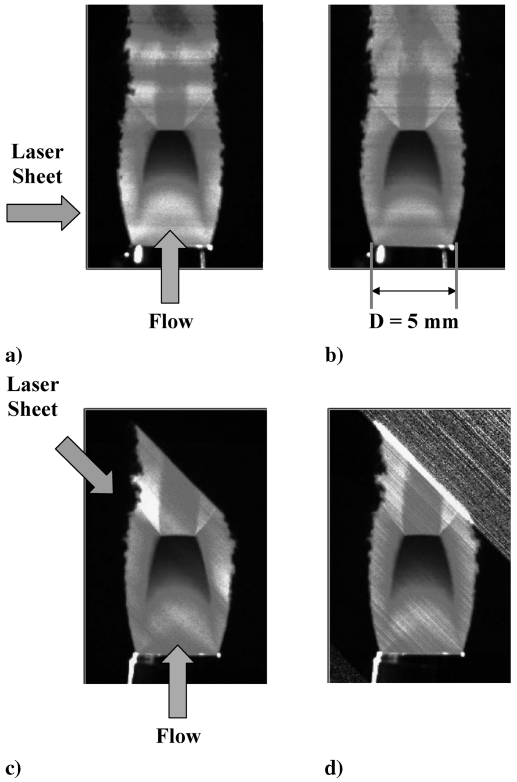

Fig. 2 NO-PLIF images obtained in an underexpanded jet near 44, 097.22 cm^{-1}; uncorrected images (left) and corrected images (right) accounting for nonuniformities in the laser sheet using an image processing algorithm; directions of the flow and laser sheet are indicated.

Image Processing

At each frequency, the spatial profile of the laser sheet was recorded simultaneously using NO-PLIF images inside the calibration cell. Using an appropriate coordinate-mapping technique for the 90- and 45-deg cases, every raw image of the flowfield was corrected for the spatial nonuniformity and intensity fluctuations of the laser beam. For a given pixel location in the flowfield, the corresponding pixel location inside the cell was chosen by tracing along the path of the laser beam. For each case, the path of the laser beam with respect to the nozzle-flowfield direction was located using the images recorded while sliding a knife edge across the laser sheet.

An experimental NO-LIF spectrum from the calibration cell (at room temperature and pressure) was constructed by integrating over an appropriately chosen region of interest. Inside the cell, the temperature (300 K) and pressure (1 atm) were known and a theoretical NO-LIF spectrum was calculated at these conditions. The division of the computed spectrum by the experimental spectrum gives a correction factor at each laser frequency. The corrected NO-LIF signal from the flowfield was then multiplied by the corresponding correction factor to construct the NO-LIF line shapes for further analysis.

Results

Figure 2 shows the uncorrected and corrected images when the angles between UV laser sheet and flow are 90 and 45 deg. Comparing Figs. 2a and 2c with Figs. 2b and 2d, respectively, the laser intensity spatial variations are accounted for and corrected fairly effectively via the image processing algorithm. The intercepting and reflecting shocks (oblique) and the Mach disk (normal shock) as well as other prominent structural features of the underexpanded flowfield are clearly evident in Fig. 2. The images have excellent signal-to-noise ratios (100 or more in the region after recompression beyond the normal shock) and spatial resolution.

Figure 3a shows the NO spectral line shapes at two centerline axial locations z. The excellent spectral resolution of our OP system is evident because the weaker $R_2(2)$ line is seen in the low-pressure region before the normal shock. Right before the Mach disk ($z/D = 1.35$), we can fit the experimental line shape well with a pressure of 0.13 atm. This fit is relatively insensitive to temperature and the pressure value is in good agreement with that reported previously [10]. The flow is recompressed after the normal shock and the collisionally broadened line shape after the normal shock ($z/D = 1.50$) is fit using a pressure of 1.35 atm; again, this value of pressure is in good agreement with that measured using N_2 CARS [10].

Figure 3b shows the calculated LIF signal intensity before and after normal shock for the 90-deg case. The relative LIF signal intensity was calculated using

$$S_{\mathrm{LIF}} \alpha f_B(T) N_{\mathrm{NO}} \frac{A}{A + Q(P,T)} \frac{1}{\Delta\omega_a \{1 + [\frac{2(\omega - \omega_a + \delta)}{\Delta\omega_a}]^2\}} \qquad (1)$$

where $f_B(T)$ is the Boltzmann fraction, N_{NO} is the number density of NO (molecules/cm^3), A is the rate coefficient for spontaneous emission (s^{-1}), $Q(P,T)$ is the collisional quenching rate (s^{-1}), $\Delta\omega_a$ is the collisional line width (cm^{-1}), ω_a is the central frequency of NO transition, and δ is the frequency shift due to pressure (cm^{-1}). We considered contributions from the $Q_2(5) + Q_{12}(5)$, $R_2(2)$ and $P_{22}(12) + P_{12}(12)$ transitions for our calculations. Pressure and temperature values along the jet centerline were obtained from N_2 CARS experiments and detailed Reynolds-averaged Navier–Stokes calculations in a similar experiment [10]. The collisional quenching rate was calculated using literature values for the quenching cross sections [15]. The exact frequencies and spontaneous emission coefficients for the above transitions were obtained from a

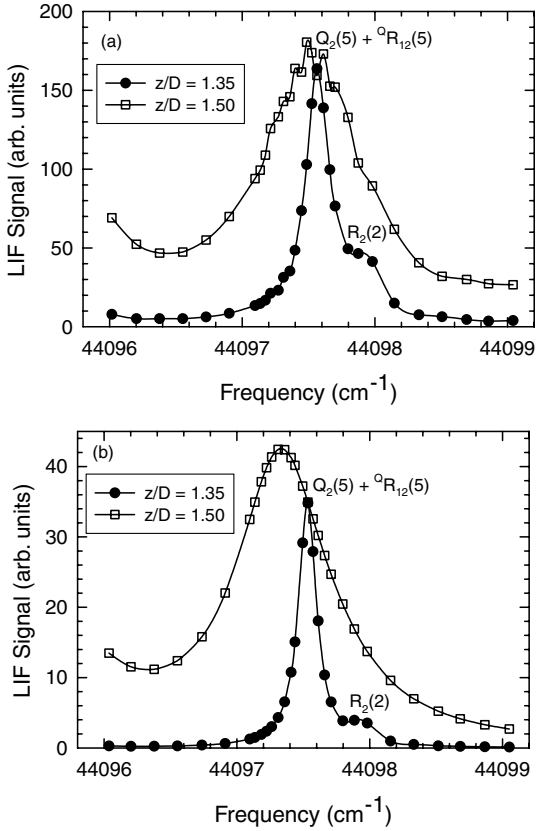

Fig. 3 Comparison between a) measured and b) calculated NO-LIF signal intensity before ($z/D = 1.35$) and after ($z/D = 1.50$) the normal shock in an underexpanded jet; part of the $P_{11}(12) + {}^{Q}P_{12}(12)$ transition is seen on the left side in the region after the normal shock ($z/D = 1.50$), in which the line shape broadens, owing to recompression.

comprehensive database for the NO *A-X* electronic system [16]. Collisional broadening and pressure shift coefficients were calculated using the best-fit expressions for absorption-line-shape data measured in a shock tube [17]. The calculated NO-LIF intensity is sensitive to temperature; however, the NO-LIF line shape is relatively insensitive to temperature. Therefore, we can fit the experimental NO-LIF spectra to obtain the collisional width, thus obtaining an accurate measurement of pressure without knowing the exact temperature. With measured values of pressure and knowing other relevant factors in Eq. (1), the temperature is determined from the ratio of LIF signal intensity across the normal shock.

A slight frequency shift between the line shapes for the 90- and 45-deg cases right before the normal shock is evident in Fig. 4. By shifting the frequency of the 45-deg curve until it best overlaps the 90-deg curve, we find that the observed frequency separation is 0.05 ± 0.01 cm^{-1}. The Doppler shift and the flow velocity are related via

$$\Delta\omega = (V/c_0)\omega_0 \cos\theta \tag{2}$$

where $\Delta\omega$ is the frequency shift (cm^{-1}), V is the flow velocity (m/s), c_0 is the speed of light in vacuum (m/s), ω_0 is the center frequency of NO transition (cm^{-1}), and θ is the angle between the laser sheet and flow direction. For the spectrum shown in Fig. 4, $\omega_0 = 44,097.53$ cm^{-1} and we calculate that $V = 480 \pm 100$ m/s before the normal shock. For a 100-K temperature, the speed of sound before the normal shock is 200 m/s. Thus, the corresponding Mach number before the normal shock is 2.4 ± 0.5. Based on the measured pressure and temperature ratios across the normal shock, the Mach number upstream of the Mach disk should lie between 2.5 and 3 for an isentropic flow.

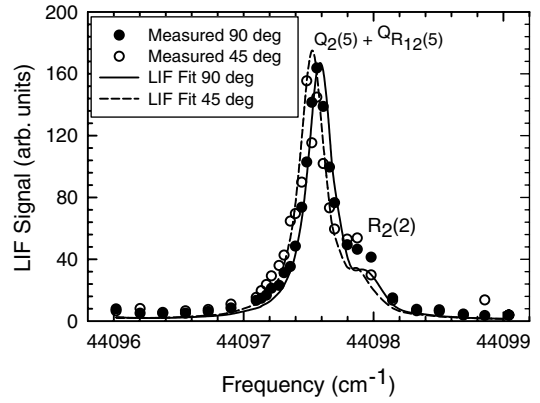

Fig. 4 Measured NO-LIF spectral line shapes in an underexpanded jet for the region before the normal shock ($z/D = 1.35$). The Doppler shift is obtained from the frequency separation between 90- and 45-deg line shapes.

Conclusions

We have demonstrated that injection-seeded optical parametric systems, which produce tunable laser radiation much narrower than commercially available dye lasers, are useful for measurements of pressure, temperature, and velocity in high-speed gas flow. Detailed images of an underexpanded jet flowfield were obtained from the fluorescence of 300 ppm NO in N_2. The images were corrected to account for the nonuniform profile of the laser sheet. The narrow line shape in the supersonic region before the normal shock was fully resolved, and we obtained good agreement between theory and experiment for a pressure of 0.13 atm for a 100-K temperature. In the same region, the bulk flow velocity determined from the measured Doppler shift is in reasonable agreement with the velocity computed assuming an isentropic expansion before the normal shock. The recompression of the flow after the shock was also captured by the measured LIF line shapes and calculated theoretical fits. The OP system and LIF techniques that we have demonstrated in this paper can potentially be used with emerging pulse-burst laser and high-frame-rate camera technology to perform instantaneous measurements of temperature, pressure, and velocity in high-speed flows.

Acknowledgments

Funding for this research was provided by the U.S. Air Force Office of Scientific Research under contract no. FA9550-04-1-0425 (John Schmisseur, Program Manager).

References

[1] Zimmermann, M., and Miles, R. B., "Hypersonic-Helium-Flow-Field Measurements with the Resonant Doppler Velocimeter," *Applied Physics Letters*, Vol. 37, No. 10, 1980, pp. 885–887. doi:10.1063/1.91784

[2] Hiller, B., McDaniel, J. C., Rea, Jr., E. C., and Hanson, R. K., "Laser-Induced Fluorescence Technique for Velocity Field Measurements in Subsonic Gas Flows," *Optics Letters*, Vol. 8, No. 9, 1983, pp. 474–476.

[3] McDaniel, J. C., Hiller, B., and Hanson, R. K., "Simultaneous Multiple-Point Velocity Measurements Using Laser-Induced Iodine Fluorescence," *Optics Letters*, Vol. 8, No. 1, 1983, pp. 51–53.

[4] Paul, P. H., Lee, M. P., and Hanson, R. K., "Molecular Velocity Imaging of Supersonic Flows Using Pulsed Planar Laser-Induced Fluorescence of NO," *Optics Letters*, Vol. 14, No. 9, 1989, pp. 417–419.

[5] Miles, R. B., and Lempert, W. R., "Two Dimensional Measurement of Density, Velocity, and Temperature in Turbulent High Speed Air Flows by UV Rayleigh Scattering," *Applied Physics B, Photophysics and Laser Chemistry*, Vol. 51, No. 1, 1990, pp. 1–7. doi:10.1007/BF00332317

[6] Elliott, G. S., Samimy, M., and Arnette, S. A., "A Molecular Filter Based Velocimetry Technique for High Speed Flows," *Experiments in Fluids*, Vol. 18, Nos. 1–2, 1994, pp. 107–118. doi:10.1007/BF00209367

[7] Herring, G. C., Fairbank, Jr., W. M., and She, C. Y., "Observation and Measurement of Molecular Flow Using Stimulated Raman Gain Spectroscopy," *IEEE Journal of Quantum Electronics*, Vol. 17, No. 10,

1981, pp. 1975–1976.
doi:10.1109/JQE.1981.1070647

[8] Herring, G. C., Lee, S. A., and She, C. Y., "Measurements of a Supersonic Velocity in a Nitrogen Flow Using Inverse Raman Spectroscopy," *Optics Letters*, Vol. 8, No. 4, 1983, pp. 214–216.

[9] Gustafson, E. K., McDaniel, J. C., and Byer, R. L., "CARS Measurement of Velocity in a Supersonic Jet," *IEEE Journal of Quantum Electronics*, Vol. 17, No. 12, 1981, pp. 2258–2259.
doi:10.1109/JQE.1981.1070736

[10] Woodmansee, M. A., Lucht, R. P., and Dutton, J. C., "Development of High-Resolution N_2 Coherent Anti-Stokes Raman Scattering for Measuring Pressure, Temperature, and Density in High-Speed Gas Flows," *Applied Optics*, Vol. 39, No. 33, 2000, pp. 6243–6256.

[11] Wu, P. P., and Miles, R. B., "High-Energy Pulse-Burst Laser System for Megahertz-Rate Flow Visualization," *Optics Letters*, Vol. 25, No. 22, 2000, pp. 1639–1641.
doi:10.1364/OL.25.001639

[12] Thurow, B., Jiang, N., Samimy, M., and Lempert, W., "Narrow-Linewidth Megahertz-Rate Pulse-Burst Laser for High-Speed Flow Diagnostics," *Applied Optics*, Vol. 43, No. 26, 2004, pp. 5064–5073.
doi:10.1364/AO.43.005064

[13] Thurow, B., Jiang, N., Lempert, W. R., and Samimy, M., "Development of Megahertz-Rate Planar Doppler Velocimetry for High-Speed Flows," *AIAA Journal*, Vol. 43, No. 3, 2005, pp. 500–511.

[14] Kulatilaka, W. D., Anderson, T. N., Bougher, T. L., and Lucht, R. P., "Development of Injection-Seeded, Pulsed Optical Parametric Generator/Oscillator Systems for High-Resolution Spectroscopy," *Applied Physics B (Lasers and Optics)*, Vol. 80, No. 6, 2005, pp. 669–680.
doi:10.1007/s00340-005-1772-y

[15] Paul, P. H., Gray, J. A., Durant, Jr., J. L., and Thoman, Jr., J. W., "Collisional Electronic Quenching Rates for NO $A^2\Sigma^+(v' = 0)$," *Chemical Physics Letters*, Vol. 259, Nos. 5–6, 1996, pp. 508–514.
doi:10.1016/0009-2614(96)00763-4

[16] Reisel, J. R., Carter, C. D., and Laurendeau, N. M., "Einstein Coefficients for Rotational Lines of the (0,0) Band of the NO $A^2\Sigma^+$–$X^2\Pi$ System," *Journal of Quantitative Spectroscopy and Radiative Transfer*, Vol. 47, No. 1, 1992, pp. 43–54.
doi:10.1016/0022-4073(92)90078-I

[17] Chang, A. Y., DiRosa, M. D., and Hanson, R. K., "Temperature Dependence of Collision Broadening and Shift in the NO A-X (0,0) Band in the Presence of Argon and Nitrogen," *Journal of Quantitative Spectroscopy and Radiative Transfer*, Vol. 47, No. 5, 1992, pp. 375–390.
doi:10.1016/0022-4073(92)90039-7

E. Oran
Editor-in-Chief